Material Science Research India Vol. **7**(2), 325-337 (2010)

Cyclic voltametric behavior of iron in 0-2 M HNO_3 solutions

N.A. AL-MOBARAK

Department of Chemistry, Faculty of Science,
Princess Nora Bint Abdurrahman University, Riyadh (Saudi Arabia).
E-mail: almobarak@yahoo.com

(Received: October 08, 2010; Accepted: November 14, 2010)

ABSTRACT

The electrochemical behavior of iron electrodes is investigated in the presence of 0.5 – 2.0 M HNO_3 solutions at 25^{0}C using cyclic voltammetric technique. The effect of cycling, scanning rate, voltage excursion and the initial starting potential was studied. An unusual anodic peak (B) in the active potential region; an oxidation peak (G) during the reverse sweep; crossing unique point "a" and hydride–oxidation step (arrest A\) characterizes the complete voltammogram. Also, the results revealed that no passivation takes place and the presence of two critical potentials namely: E_c and E_d. Below E_c (during the lower potential region) hydrogen evolution reaction occurs and above E_d (during the higher potential region) oxygen evolution reaction occurs.

Key words: Cyclic voltammetry; iron, HNO_3; electrochemical behaviour.

INTRODUCTION

The electrochemical behavior and mechanism of iron and steel dissolution in HCl and H_2SO_4 acid solutions have been studied extensively[1-12]; perhaps more widely than in HNO_3. Most investigations of iron and steel corrosion in nitric acid solutions of various concentrations were carried out using different techniques namely, the impedance method[13], the thermometric technique[14, 15], the galvanostatic cathodic and anodic polarization measurements[16] and weight loss experiments[17]. Apparently, no work on iron in dilute HNO_3 solutions ($\leq$ 2.0 M) has been done using cyclic voltammetry. However, the situation is still unclear and needs more clarification.

It is generally accepted that in concentrated HNO_3 solutions ($\geq$ 10 M), passivation of iron and steel takes place[14,18] through the formation of γ-Fe_2O_3 or an oxide overlying a H-layer on the surface of the metal[19, 20]. On the other hand, in dilute HNO_3 solutions vigorous corrosion occurs at considerably higher rate than that measured in concentrated HNO_3 solutions or in any other strong acid of comparable concentration[21-23]. Moreover, it was reported that[13] a protective film of n-type semiconductor phase could be formed in the low potential range and could be converted to a metal-like layer at high potentials.

In the present work, the electrochemical behavior of pure iron electrodes in 0.5 – 2.0M HNO_3 solutions were studied thoroughly using cyclic voltammetric technique. This could give further insight into this issue and a better understanding of dissolution and corrosion behavior of the iron / HNO_3 system.

EXPERIMENTAL

Iron electrode (99.99 %, Aldirch Chemicals) of apparent surface area of 0.50cm^2 was used as a working electrode. Before each experiment, a fresh iron electrode surface was treated by abrading the electrode with a different grade emery paper, degreased with acetone and then rinsed with doubly distilled water. The

electrolyte HNO_3 solutions were prepared from analytical reagent (Merck) and doubly distilled water.

A conventional three electrode glass cell containing iron working electrode, a platinum counter electrode (separated from the cell solution by a sintered glass frit) and a reference saturated calomel electrode (inside a luggin-s capillary probe) was adopted for the cyclic voltammetry experiments. The base surface of the working electrode was always kept in close touch with the luggin capillary tip to minimize the IR drop through the cell.

Prior each experiment, the iron electrode was cathodically pretreated at the hydrogen evolution potential (–1.80 V) for 10 min to remove any air-formed oxides. Then the electrode potential was hold constant at the open circuit potential (–0.85 V) for 5 min after which the experiment is swept in the potential range –1.80 to 2.50 V. This would lead to minimize the influence of hydrogen gradient on the oxidation process and to produce same initial surface condition as well as good reproducibility of the results.

The cyclic voltammetry experiments were performed using a Weaking potentiostat (model pos 73) and the voltammograms were plotted on X – Y recorder type pL 3.

RESULTS AND DISCUSSION

General features

Fig. 1 presents a family of the cyclic voltammogram curves of the cathodic pre-treatment iron electrodes in 0.5 – 2.0 M HNO_3 solutions traced between the negative potential limit (– 1.80 V) to the positive potential limit (+ 2.50 V) vs. SCE at a scan rate of 25 mV s^{-1} and 25°C. Evidently, all the curves have the same general shape. The forward half-cycle of the voltammogram consists of four well-defined regions namely, region A (with its characteristic arrest A\); peak B; arrest C and oxygen evolution (region D). The backward half-cycle consists of four well-defined regions, namely, region E; arrest F; inverted oxidation peak G and reduction region H (with its associated two waves M and N).

For simplicity and clarity, the cyclic voltammogram curve shown in Fig. 2, which was recorded for iron electrode in 1.0 M HNO_3 solution is selected as a typical voltammogram that could be used for the subsequent detailed discussion.

Inspection of the cyclic voltammogram of Fig. 2 reveals the presence of four sections of phase-polarization, which are designed as (I, II, III and IV). These sections corresponding to the potential regions (– 1.80 to – 0.312 V), (– 0.312 to 0.20V), (0.25 to 1.52 V) and (1.52 to 2.50 V), respectively. In order to be able to explain the mechanisms and kinetics of the various features observed in the voltammogram of Fig. 2, the following additional studies including cycling, potential scan rate, reversing potential and staring potential effects were carried out.

Effect of cycling

Fig. 3 shows three successively repeated sweeps of the cyclic voltammograms of iron electrode in 1.0 M HNO_3 solution traced between – 1.8 and + 2.5 V vs. SCE at a scan rate of 25 mV s^{-1} and 25°C. Evidently, cycling has practically no significant effect on the shape of the characteristic voltammogram. However, in the successive cycles, there is only a noticeable shift in the potential of region A towards more negative direction. All these results would indicate that the initial state of the electrode surface is practically the same for the three repeated sweeps.

Effects of various scan rates

Fig. 4 illustrates the effect of sweep rates in the range of 25 – 100 mVs^{-1} on the cyclic voltammograms traced for iron electrode between – 1.8 and +2.5 V vs. SCE at 25 °C. Evidently, increasing scanning rate leads to some minor change as indicated by slight change in the current density of the cathodic region H (with its characteristic two waves M and N), with no effect on its potential. Apart from this minor change, increasing scan rate has practically no effect on the potentials and current densities of all the anodic features.

Effect of reversing potential

In order to correlate the anodic and cathodic polarization features, a series of voltammetric sweeps with different chosen reverse potentials were considered. The results are shown

in Fig. 5 (a – d). When the direction of potential was reversed at the vertex (see Fig. 5d) and by analogy with similar studies, non of the normally and generally associated processes (i.e. reduction features), which could be expected was observed. Instead, the current remains high in the anodic section over the whole potential region up to the crossing point "a". Also, region E, arrest F and the inverted anodic peak G as well as the reduction region H (with its characteristic two waves M and N) were observed at the extreme negative potential. This would indicate that any film or layer that was previously formed during the previous anodic polarization were either immediately dissolved or were in poor contact with the electrode surface. Hence, the cyclic voltammogram curve of Fig. 5d (i.e. complete voltammogram) could be visualized as divided into two well-defined parts (above and below the basic line) with its characteristic potential at point "a" (E_a = – 0.312 V). Thus, in the cathodic region (i.e. below the basic line), the curve consists of the "phase-polarization section I" while in the anodic region (i.e. above the basic line), the voltammogram consists of the three different "phase-polarization sections II, III and IV". In other words, the basic line with its characteristic crossing point "a" divided the voltammogram into two well-defined voltammograms above and below base line.

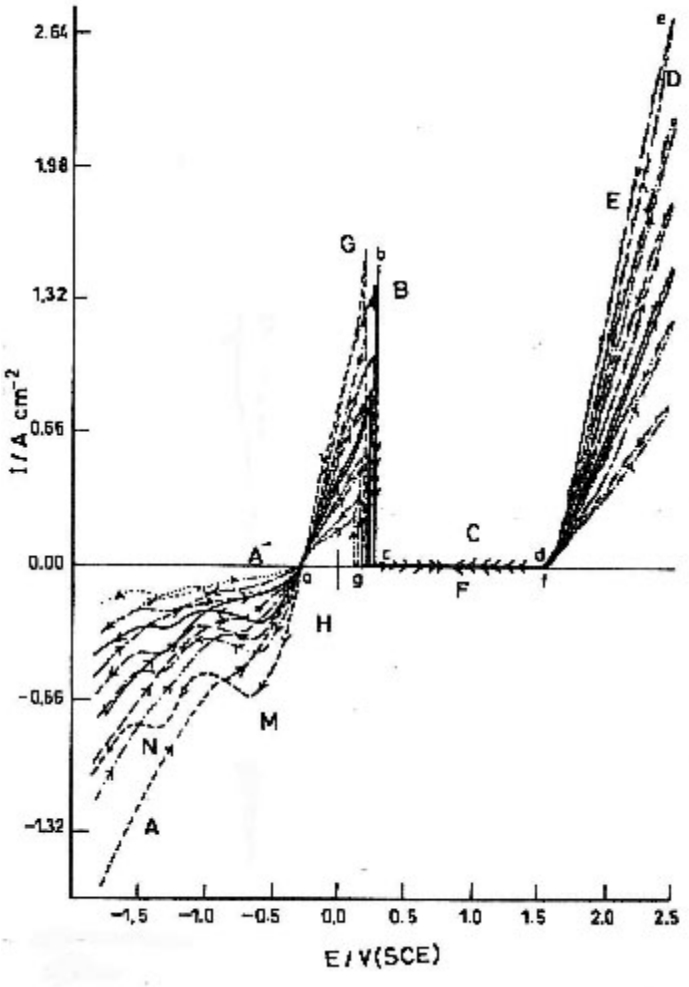

Fig. 1: Cyclic voltammograms of iron in HNO_3 of different concentrations at scan rate of 25 mV sec^{-1} and 25°C; (...) 0.50 M, (-..-) 0.75 M, (-) 1.00 M, (- -) 1.25M, (-×-) 1.50 M and (- -) 2.00 M

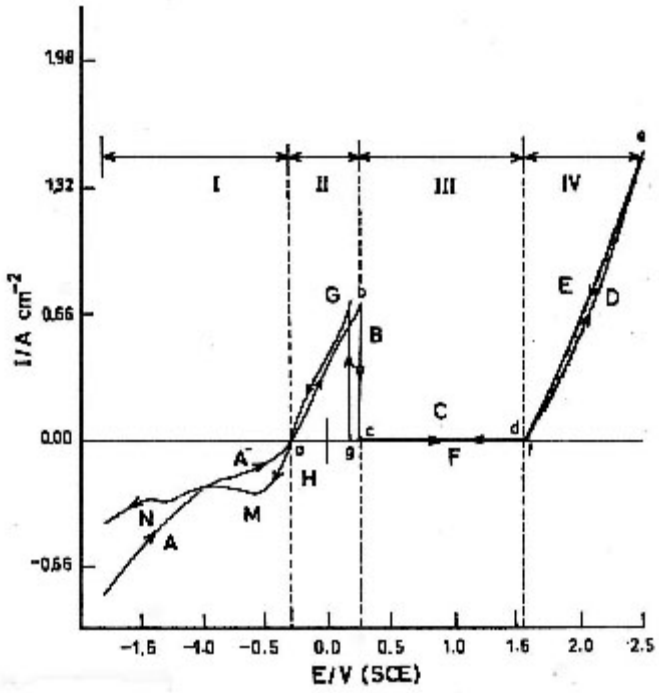

Fig. 2: Four phase polarization potential regions of the anodic forward and the cathodic backward of iron in 1.00 M HNO_3 solution

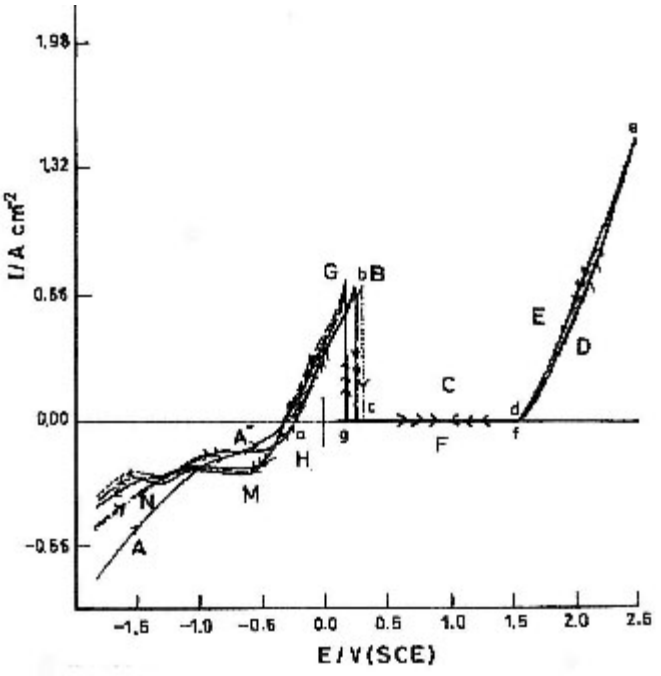

Fig. 3: Three successive sweeps of iron electrode in 1.00 M HNO_3 solution at scan rate of 25 mV sec^{-1} and 25°C; (-) first sweep, (--) second sweep and (...) third sweep

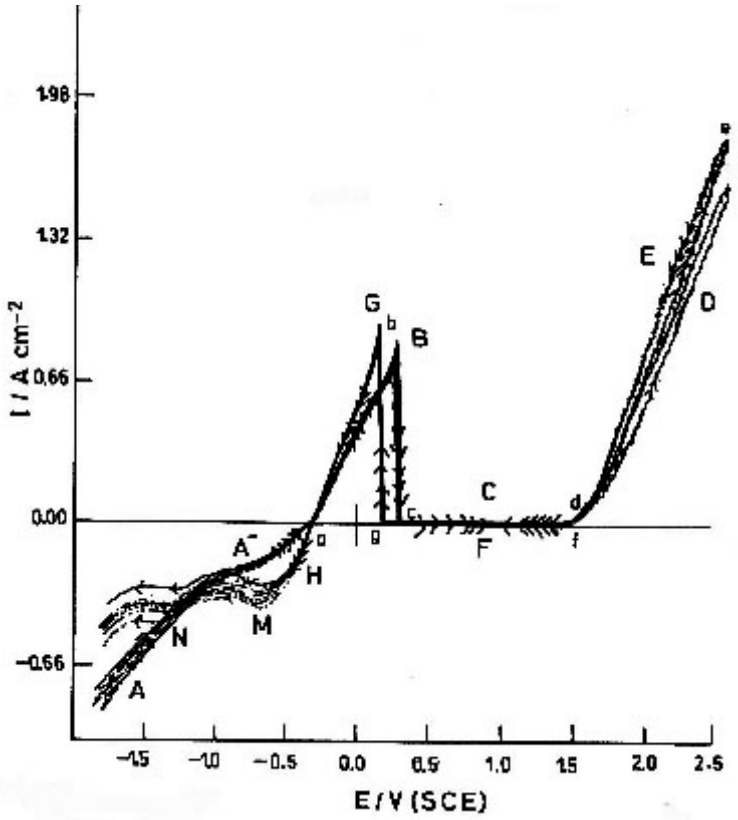

Fig. 4: Cyclic voltammograms of iron in 1.00 M HNO_3 solutions at different sweep rates: (-) 25 mV sec^{-1}, (-.-) 40 mV sec^{-1}, (-) 55 mV sec^{-1}, (...) 70 mV sec^{-1}, (-...-) 85 mV sec^{-1} and (....) 100 mV sec^{-1}

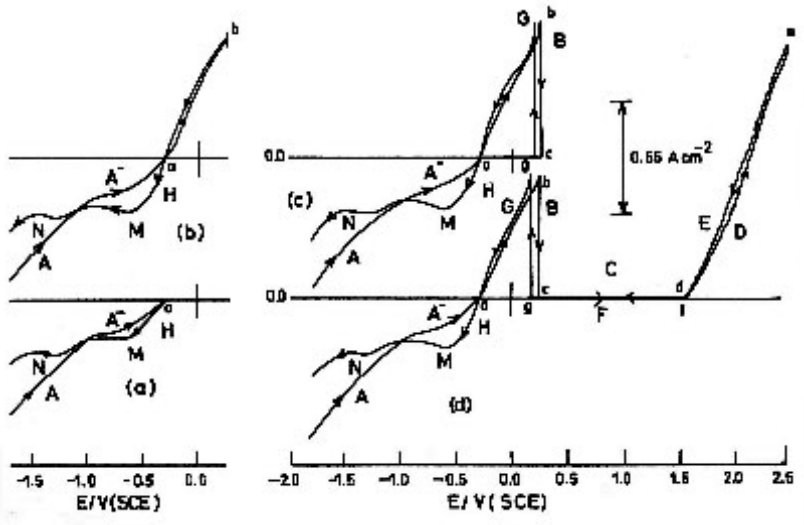

Fig. 5: Effect of increasing anodic reversal potential on iron electrode in 1.00 M HNO_3 solutions at sweep rate of 25 mV sec^{-1} and 25°C

Apparently, one would think from the cyclic voltammogram of Fig. 5d that peak B is correlated to region A (with its characterstic arrest A\) and that peak G is correlated to region H (with its characteristic two waves M and N). However, critical inspections of the cyclic voltammograms of Fig. 5 (a – d) show clearly that both region A (with its characteristic arrest A\) and region H (with its characteristic two waves M and N) are exactly the same. This difficulty disappears, however, when the cyclic voltammogram curve of Fig. 5a is critically examined. Evidently, region A (with its characteristic arrest A\) is correlated to region H (with its characteristic two waves M and N). It could be concluded that above and below the basic line, the two voltammograms are essentially separate. Point "a" can be considered as a transition point between the two separate voltammograms. In other words,

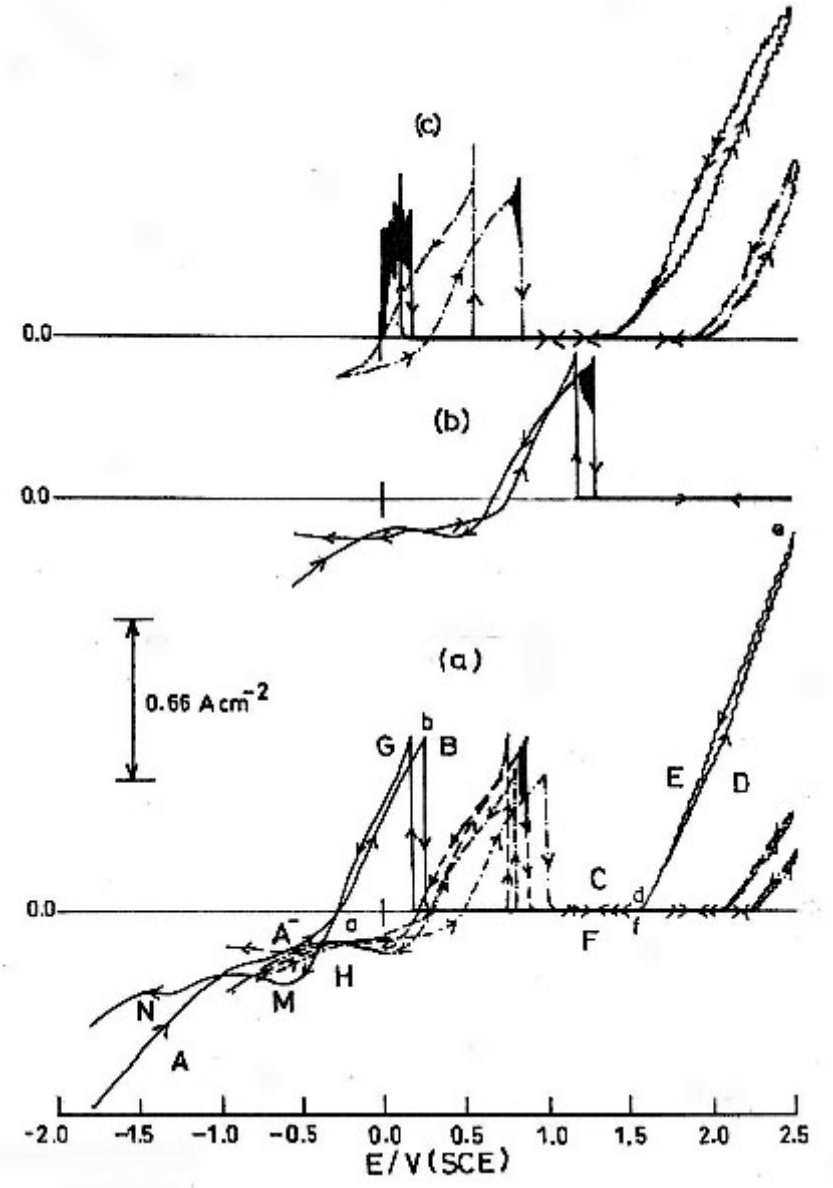

Fig. 6: Cyclic voltammograms of iron electrode in 1.00 M HNO_3 solutions obtained with different starting potential at sweep rate of 25 mV sec^{-1} and 25°C. a: (-) at –1.80 V, (--) at –1.00 V and (-.-) at – 0.75 V. b: (-) at – 0.50 V and c: (-.-) at – 025 V and (¾) at 0.00 V

the upper anodic voltammogram is not correlated to the lower cathodic voltammogram. The anodic voltammogram is a function of the previous cathodic polarization.

Critical inspection of all the voltammograms of Fig. 5 (a – d) reveals that, the potential at the crossing point "a" (– 0.312 V) is the same. These results would indicate that the potential at point "a" has different definitions. With respect to the above (anodic) voltammogram, the potential at the crossing point "a" represents both the initial and end of it. With respect to the below (cathodic) voltammogram, the potential at crossing point "a"

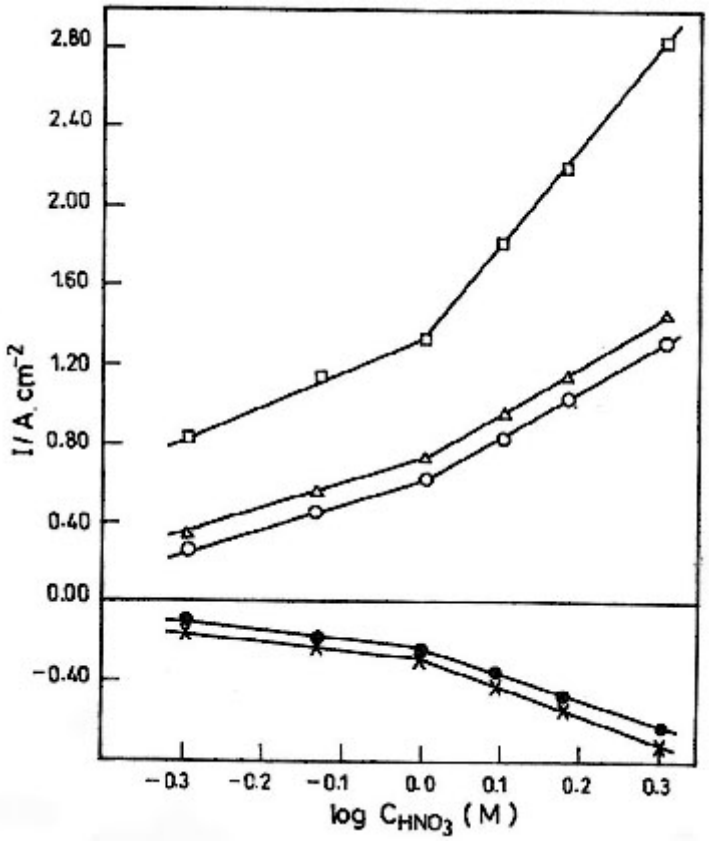

Fig. 7: Dependence of the current density on log concentration of HNO_3 for the various anodic and cathodic features of iron electrode; (–o–) at the potential of peak B, (–Δ–) at the potential of peak G, (-□-) at the potential of the vertex, (– –) at the potential of peak M and (–x–) at the potential of peak N

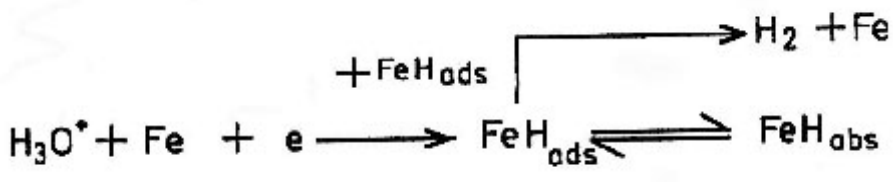

Fig. 8: The oxidation of adsorbed and absorbed hydrogen that had been produced during the cathodic (hydrogen charging) pretreatment

represents the end of region A as well as the beginning of the cathodic region H (with its characteristic two waves M and N). Consequently, point "a" could be considered as a transition point between the two sections of the voltammogram.

When the potential was reversed beyond the anodic peak B, the anodic peak G was observed directly at point "g" (E_g = – 0.200 V) during the reverse sweep (see Fig. 5c). This gives an indication for great similarity between anodic peak B and the inverted anodic peak G (this is further discussed below). However, peak G is at slightly more negative potential than peak B because the needs to dissolve the protective film during the reverse sweep.

Effect of starting potential

Cyclic voltammograms with the same return potential (+ 2.50 V) but varying starting potentials at the same scanning rate (25 mV sec^{-1}) are shown in Fig. 6 (a – c). In order to have the same starting iron electrode surface for different starting potentials, cathodic pre-treatment was carried out in the same manner as stated before. It is very interesting to state that the anodic peak B and oxygen evolution varies in magnitude with the variation of hydrogen charging conditions. In other words, the initial cathodic polarization region (i.e. region A with its characteristic arrest A\) seems to be important factor and plays an important role on the anodic reactions.

The cyclic voltammogram curve recorded at starting potential of – 0.50 V (see Fig. 6b) is of particular interest, as it shows no oxygen evolution at the end of the forward half-cycle. With increasingly more negative starting potentials than – 0.50 V (see Fig. 6a), there is a noticeable increase in the height of the anodic peak B and its shift to more negative values. In addition, there is a significant shift in the potential at point "d" (E_d = 1.52 V) into less positive value, in which a noticeable gradual increase in the oxygen evolution was observed. The same behavior was observed with increasingly more noble starting potentials than – 0.500 V (see Fig. 6c). These experimental findings would indicate the presence of a correlation between region A and the anodic peak B. Also, a correlation between the anodic peak B and the inverted anodic peak G as well as the oxygen evolution region is evident.

Also, it is observed from the cyclic voltammograms curves of Fig. 6 (a – c) that, the potential at the crossing point "a" is shifted in the noble direction by changing the starting potential either into more negative or more noble values than – 0.500V, while the potential span of arrest C is constant. This would indicate that arrest C is considered as a steady state separate potential region.

Effect of HNO_3 concentration

Increasing HNO_3 concentration produce a

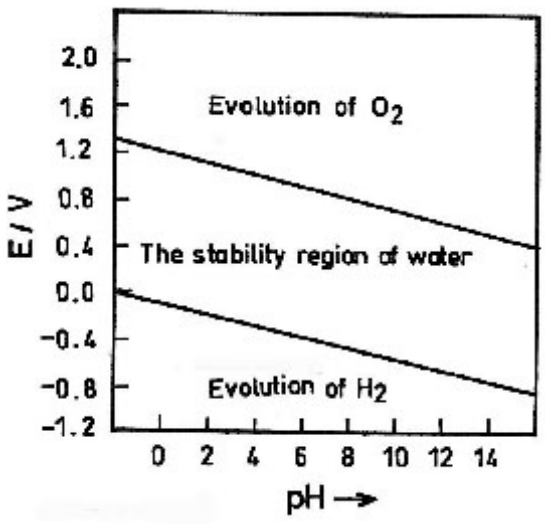

Fig. 9: The equilibrium potential difference of oxygen – hydrogen cell (taken from reference 24)

number of affects (see Fig. 1). First it raises the overpotential associated with hydrogen evolution reaction along region A. The same concentrations also causes an increase in the current density of the two peaks B and G as well as that at the vertex potential. Also, it affects the current densities of the two waves M and N in region H without changing their characteristic potentials. On the other hand, no effect was observed on the current density along the two arrests C and F.

The above mentioned variations in the current density are plotted verses log C of HNO_3 (see Fig. 7). Evidently, two distinct linear portions of different slopes characterize each curve of Fig. 9 with a definite break at 1.0 M HNO_3 solution. This finding gives an indication for the presence of a change in the mechanism of hydrogen evolution reaction. Two alternatives might be thought off as account for this behavior. The first assumes a change in mechanism is due to the sudden change between activation and concentration overpotential (i.e. change in the dissoltuion mechansim with overpotential or change in the surface state during the dissolution process). The second alternative is based on the idea that the changes from electrochemical to chemical desorption of the hydrogen gas evolution.

Mechanisms

The cyclic voltammogram of iron in 1.0 M HNO_3 solution shown in Fig. 2, indicates the presence of a clear four phase-polarization sections (I, II, III and IV) in the potential range – 1.80 V to + 2.50 V. Moreover, the complete voltammogram consists of two well-defined and distinct voltammograms above and below the basic line, respectively. Correlation between the characteristic features, which observed in the voltammogram of Fig. 2 can be sought from the above mentioned data in Figs. 5 and 6. To discuss the mechanisms and for the sake of simplicity, each of the features observed in the present system (i.e. 1.0 M HNO_3) will be interpreted separately.

The forward half-cycle

The forward half-cycle of iron voltammogram (Fig. 2) begins at the very high negative potential ($E_{starting}$ = – 1.80 V) and scanned in the anodic direction to the very high positive potential (E_{ending} = + 2.50 V). It consists of an initial region A (with its characteristic arrest A\) followed by peak B; arrest C and oxygen evolution at region D. Region A is characterized by an initial linear current rise leading to a short current arrest A\ just prior to crossing of the basic line. Along this region, the current is pure cathodic. This current will flow until the potential becomes sufficiently high to affect the crossing of the base line at the potential of point "a" (E_a = – 0.312 V). At the beginning of region A ($E_{starting}$ = – 1.80 V), the cyclic voltammogram curve starts with free iron surface, eventually with some adsorbed and absorbed hydrogen as the result for the pre-cathodization treatment. Consequently and by analogy with similar studies, the rising part of region A could be due to the decay of any cathodic processes as well as to the activation of the electrode surface. Moreover, it could be also related to the oxidation of the adsorbed and the absorbed hydrogen in the form FeH_x, which diffused out from the metal lattice. It is well known that, iron has the ability to absorb hydrogen and may be taken into solid solution or form iron hydrite (FeH_x). As illustrated in Fig. 8, the absorption can provide an alternative reaction path to the desorption of H_{ads} as H_2 gas. The appearance of arrest A\ in region A before the basic line gives an indication for the presence of slow diffusion mechanism. Consequently, the formation of the second reaction in region A is most probably due to the diffusion of FeH_x out from the metal lattice and its oxidation. Hence, the most probable explanation of arrest A\ is that the slow diffusion of the hydride oxidation step unable to remove the accumulated species from the surface fast enough to keep up with the rapidly increasing potential leading to a limiting diffusion control mechanism. As the result of the hydride oxidation step (arrest A\) with its limiting diffusion process, the solution composition adjacent to the iron electrode surface becomes high enough in the concentration of Fe^{2+} and H^+ ions. Therefore, at the potential of the crossing point "a" (corrosion potential at zero current), the upper (anodic) voltammogram started.

Beyond the crossing point "a", the anodic current density rises linearly to a maximum value (point "b", i_b = 0.58 A/cm^2) and then suddenly falls practically vertically to null value at the potential of point "c" (E_c = + 0.250 V) thus producing unusual

right angle triangle peak B. Moreover, it is of importance to remark that, visible gas started to evolve along the rising part of the anodic peak B and becomes vigorous at the maximum of peak B at which an unusual practically vertical drop in the current density takes place at $E_b = E_c = + 0.250$ V.

The easiest way to find out the most probable explanation for the mechanism of peak B is to build up a case in support of a particular electrode reaction mechanism, one has to take several criteria together and let each contribute something to narrowing the possibilities of path toward one. In this case, the following four possible trials could be taken into consideration:

(i) It is well established that metal, which is susceptible to passivation should produce a main anodic peak of "tripartite" region type namely: active-dissolution; active-passive transition and the passive state. Comparing the characteristic of the anodic peak B (see Fig. 2) with that of similar normal cases, it could be concluded that, the anodic peak B consists of an active-dissolution region only. Therefore, the anodic peak B does not show active-passive transition and no passivation regions.

(ii) There are reasons to believe that the theory of retarded mechanism could be used to describe the normal or usual anodic dissolution of metals. Consequently, if ionization of the metal is assumed to be the limiting stage in the dissolution process in the present experimental condition then the rate of the anodic process (i_a) must be exponential function of the potential according to: $i_a = K\exp[(\alpha n \varphi_a F) / (RT)]$ and the rate of anodic dissolution, as a function of the potential, can be described by Tafel equation. Since the rising part of the anodic peak B is characterized by initial linear current rise and not exponentially, thus the theory of retarded mechanism can not applied to interpret the anodic peak B.

(iii) Bringing the iron and steel into the passive state with the acid HNO_3 may be the consequence of either an increased effectiveness in the cathodic process or a reduced rate of the anodic process. Critical inspection of the present results revealed that NO_3^- ions are not reduced at significant rate and the present current is incapable of shifting the potential to values where film cause active-passive and passivation begins to form.

(iv) In the present study, the potential at the crossing point "a" ($E_a = -0.312$V) can be considered as the beginning of the main upper (anodic) voltammogram. This would suggest that the unusual linear rising part of the anodic peak B is associated with the concentration of $Fe^{2+}$and H^+ that formed during oxidation of FeH_x along cathodic region A. Moreover, the evolution of gas along the rising part of peak B appears somewhat unusual. This difficulty disappears, however, when the complementary cathodic reaction is taken into consideration. It seems that the hydrogen ions produced from the oxidation of FeH_x are combined to form H_2 gas on the cathodic sites. Moreover, thermodynamic data presented by Pourbaix indicates that only the Fe^{2+} species are stable within the potential range up to the anodic peak B. It follows that, no active-passive transition associated with the anodic peak B and thus no change of Fe^{2+} to Fe^{3+} species. In other words, no passive region.

Following the above discussion it could be concluded that the most probable controlling mechanism of peak B could be attributed to the chemical change composition of solution at the metal interface at the potential of point "a" due to the liquid concentration of Fe^{2+} and H^+ as the result of the hydride oxidation step in previous cathodic polarization. It follows that the rise of the anodic dissolution rate at the beginning of peak B is rather complex and is due to the simultaneous oxidation of metal producing hydrates oxide precipitate (i.e. $Fe(OH)_2$) on the active anodic sites of the electrode and the adsorption of H_2 molecules at the active cathodic sites. When the iron surface is completely covered with both $Fe(OH)_2$ and adsorbed H_2 molecules, the anodic dissolution current density falls suddenly at E_b to practically null value at E_c ($E_b = E_c = + 0.25$ V) due to the formation of a complete surface film barrier at peak B. Moreover, the most probable HER during the rising part of the anodic peak B is due to the discharge of hydrogen ions

forming MH followed by a chemical discharge of H_2. This is supported by the fact that the unusual sudden fall of the current density at E_b is the result of EC mechanism (electron charge "D" followed by chemical desorption "CD") according to:

$$H_3O^+ \rightarrow MH \leftrightarrow H_2 \quad ...(1)$$

or

$$H_3O^+ \leftrightarrow MH \rightarrow H_2 \quad ...(2)$$

The results revealed that, the potential at point "c" (E_c = + 0.25 V) is equal to the potential at point "b' and independent on the acid concentration. Below this specific potential the protective film is unstable and can undergo dissolution, in which the activated peak G is developed (further discussion will be given below). At the potential of point "c" the current density drops to practically null value. This would indicate that the observed potential is a thermodynamically hydrogen equilibrium potential. Such a situation arises when electronation and de-electronation directions are at the same rate (i.e. net i is zero). Thus, the potential at $E_b = E_c$ is an equilibrium potential of the corroded metal H^+ / H_2 system. This hydrogen equilibrium potential is slightly nobler than the redox couple at platinum. Such apparent discrepancies in comparison with that (pt /H^+, H_2) because it is associated with corroded iron system against platinum.

There is another situation at which the result current could be observed. It may be that the de-electronation current of the given electrode reaction may be equalized by the electronation current of another different reaction. Under this condition what is observed is not an equilibrium potential as before, but a steady state mixed potential set up by two the different reactions, most probably the anodic iron dissolution and the hydrogen deposition. It follows that, at more oxidizing potential than E_c, the iron electrode acquires more stability and / or thickness, in which the formation of iron oxide is continued. Consequently, the equilibrium condition at E_c is transformed to a steady state condition along the arrest C. At the end of arrest C and at the potential of point "d" (E_d = 1.52 V), oxygen begins to evolve and becomes vigorous along the region D. This would indicate that at E_d, oxidation of H_2O molecules producing O_2 gas onto the oxide-covered electrode surface areas according to:

$$2\ H_2O = O_2 + 4\ H^+ + 4\ e \quad ...(3)$$

and the anodic dissolution takes place within its pores.

The backward half – cycle features

On reversing the scan at the vertex potential (E_{vertex} = + 2.50 V), the backward half-cycle starts (see Fig. 2). Evidently, the current remained high in the anodic section and then decreases to the potential of point "f" ($E_f = E_d$ = 1.52 V) producing region E. The backward region E is similar to the forward region D. These two regions (D and E) form together the hystresis oxygen loop. This would indicate that when the scan was reversed, there were still some accumulated products of the electrolyte at the interface. Moreover, the existence of this descending branch of the oxygen hysteresis loop (region E) could be attributed to the reverse reaction of the previously of oxygen evolution reaction along region D according to:

$$O_2 + 2\ H_2O + 4\ e = 4\ OH^- \quad ...(4)$$

Furthermore, the results revealed that, the potential of point "f" coincides with that of point "d" of the forward scan. Thus, at the potential of point "f" the steady state electrode condition starts by two reactions.

The current arrest at F for the backward direction coincides with that of the forward direction (arrest C) and slightly longer than it indicating that the two regions (F and C) are practically the same.

The current along arrest F flows until the potential becomes sufficiently negative enough at point "g" (E_g = – 0.200 V). At this potential, the current density rises suddenly to a maximum value then starts to decrease to the potential of point "a" (E_a = – 0.312V), thus producing peak G in anodic direction. Peaks G and B are both oxidation processes occurring at approximately same potential (actually peak G is at a more negative potential than peak B by about 50 mV). However, they are separated only because they appear at different time in the voltammogram. Moreover, the same charge magnitude is associated with them.

This would indicate that, the flow of initially high current at the potential of point "g" is soon shifted by the action of oxidizing agent or as the result of limited solubility of the product at the maximum of peak G after which the current starts to decrease towards the potential of the crossing point "a". It flows that, the inverted anodic peak G is developed by dissolution / precipitation cycle taking place at E_g, in which an oxide modified stable, is formed under the new prevailing condition. Moreover, a certain amount of adsorbed H_2 previously formed during the anodic sweep would be still on the electrode surface.

The inverted anodic peak G ended at point "a" potential ($E_a = -0.312$ V) with a high concentration of Fe^{2+} and H^+ ions at the metal interface. Thereafter, the beginning of the main cathodic region H (with its associated waves M and N) was observed. Thus, the crossing point "a" is considered as unique point potential. The results of Figs. 1 and 5 revealed that, the position of the unique point at point "a" ($E_a = -0.312$V) is practically not affected by the HNO_3 concentration and the scanning rate. This would indicate that at the unique point, the metal surface has the same function and plays the same role. The conclusion could be drawn from this observation would be that, over the whole concentration range (0.50 – 2.00 M) and at the unique point "a", MH is present during the forward half – cycle as well as during the backward half – cycle. The fact that the crossing point "a" is the initial and final of the well-defined the two (upper and lower) voltammograms is strong evidence that each voltammogram depends on the chemistry – solution structure of the system at the potential of the crossing point "a".

The cathodic region H (the reduction region) is characterized by the presence of two cathodic waves M and N at potentials – 0.625 V and – 1.280 V, respectively (see Fig. 2). At the end of the voltammogram ($E_{end} = -1.80$ V) H_2 evolution was observed. Moreover, it is observed that the difference in the potentials of the two cathodic waves M and N amounts to 0.655 V, which is in good agreement with that between Fe / H and H / H_2 system. Also, the quantity of electricity consumed along the two cathodic waves (M and N) are found to be practically of the same magnitude. These findings would reveal that, along the cathodic wave M the discharge of H^+ ions forming adsorbed hydrogen atoms takes place. This is followed by electrochemical desorption into H_2 gas along the cathodic wave N.

From the foregoing discussion it is illustrated that H_2 is formed during both the rising part of the anodic B and the cathodic region H by first discharge of H_3O^+ (D) followed by either chemical desorption (CD) or electrochemical desorption, respectively. Moreover, the whole cyclic voltammogram (see Fig. 2) could be pictured as consists of three parts with two critical potentials at E_c and E_d. Below E_c hydrogen electrode reactions occurs, while above E_d oxygen evolution occurs and the equilibrium potential of both are independent on HNO_3 concentration. This picture of the complete voltammogram can be considered as equivalent to the $H_2 - O_2$ cell [24] as indicated in Fig. 9.

However, one of the major aims of the electrochemical technology is to produce an electrode, in which the substrate is less expensive than pt, possess good electrochemical resistance to the reaction environment and is metallically conducting. This appears to be promising in this respect when prepared under the present experimental conditions those of Fe as substrate for H_2 and O_2.

CONCLUSIONS

The voltammograms of iron electrodes in 0.50 – 2.0 M HNO_3 solutions display several interesting features during both the forward and backward half – cycles. The over all cyclic voltammogram could be looked upon in several ways. First it consists of four distinct phase-polarization sections (namely: I, II. III and VI). Another picture is that the basic line with its characteristic crossing point "a" divides the over all voltammogram into two well (upper and lower) voltammograms. A third picture reveals that the over all voltammogram consists of three distinct regions namely, hydrogen evolution section (during the lower potential region), oxygen evolution section (during the higher potential region) separated by a steady-state-potential region for water stability. This picture of complete voltammogram can be considered as equivalent to the $H_2 - O_2$ cell.

REFERENCES

1. J. O' M Bockris, D. Drazic and A. R. Despic, *Electrochim. Acta* **4**: 325 (1961) .
2. Z. A. Foroulis and H. H. Uhlig, *J. Electrochem. Soc.* **12**: 1177 (1965).
3. L. Felloni, *Corros. Sci*. **8**: 133 (1968).
4. K. Sugimoto and Y. Sawada,*Corros. Sci*. **17**: 425 (1977).
5. K. C. Pillai and R. Narayan, *J. Electrochem. Soc*. 125: 1393 (1978).
6. K. C. Pillai and R. Narayan, Corros. Sci. 23 (1983) 151.
7. W. J. Lorenz and K. E. Heusler, "Corrosion Mechanisms", edited by F. Mansfeld, (Marcel Dekker, Inc., New York, 1-83(1987).
8. J. O'M. Bockris and B. Yang, *J. Electrochem. Soc*. **138**: 2237 (1991).
9. M. Bojinov, I. Betova and R. Raicheff, *J. Appl. Electrochem.* **26**: 939 (1996).
10. X. L. Cheng, H. Y. Ma, J. P. Zhang, X. Chen, S. H. Chen and H. Q. Yang, *Corrosion* **54**: 396 (1998).
11. M. S. Morad, *Corros. Sci*. **42**: 1307 (2000).
12. A. A. Hermas, M. S. Morad and M. Wahdan, J. *Appl. Electrochem*. **34**: 95 (2004).
13. X. Gue, Y. Tomoe, H. Imaizumi and K. Katoh, *J. Electroanal. Chem.* **449**: 95 (1998).
14. A. M. Shams El-Din and M. Y. Fakhr, *Corros. Sci.* **14**: 615 (1974).
15. B. Sanyal and K. Srivastava, *Corros. Sci.* **12**: 689 (1972).
16. A. K. Mohamed, K. M. Ibrahim and M. N. H. Moussa, *Anti-corrosion* 4 (1989).
17. F. Balband, G. Sanchez, P. Fauvet, G. Santarini and J. Picard, Corros. Sci. 24 (2000) 1685.
18. K. F. Bonhoeffer, *Corrosion* **11**: 304t (1955).
19. L. Tronstad and W. Brogmann, *Trans. Faraday Soc*. **30**: 349 (1934).
20. R. Porshad and I. C. Verman, *J. Phys. Chem.* **16**: 154 (1948).
21. N. Shikai and L. Yufen, "Corrosion Inhibition", edited by R. H. Hausler (Proceeding of the International of Corrosion Inhibition, National Association of Corrosion Engineers, Texas, 48-54 (1988).
22. N. D. Tomashov, "Theory of Corrosion and Protection of Metals", edited by B. Tytell, I. Geld and H. Preiser (The Machillan Company, New York, 507-513 (1966).
23. U. R. Evsns, "An Introduction to Metallic Corrosion", Edward Arnold (Publisher) LTD (London) 57-60 (1963).
24. J. O'M. Bockris and A. K. N. Reddy, "Modern Electrochemistry", Volume 2, Plenum press (New York) 1121-1123 (1974).